$$\mathbf{M} \overset{\text{odeling}}{\underset{\text{athematical}}{\mathbf{MC}}} \overset{\text{omputing}}{}$$

Maxwell fluid flow in system supplying hydrodynamically active polymer to boundary layer of streamlined object

Pogrebnyak V. G.[1], Pogrebnyak A. V.[2], Perkun I. V.[1]

[1]*Ivano-Frankivsk National Technical University of Oil and Gas,*
15 Karpatska Str., 76019, Ivano-Frankivsk, Ukraine
[2]*University of Customs and Finance,*
2/4 Volodymyr Vernadsky Str., 49000, Dnipro, Ukraine

The article presents the results of the numerical simulation of the Maxwell fluid flow in the system supplying hydrodynamically active polymer in the boundary layer of a streamlined object. The case of slow flow is considered. In this case, the inertial terms can be neglected, the velocities, stresses, and stream functions can be written as the decomposition by Weisenberg number, and we can assume that the Weissenberg number is less than one. The established features of the behaviour of the Maxwell fluid flow with a longitudinal velocity gradient and the manifestation of the effects of elastic deformations are crucial for understanding processes taking place in the system supplying hydrodynamically active polymer in the boundary layer of a streamlined object. Understanding the nature of the effects of elastic deformations in the supplying system makes it possible to offer a hydrodynamic calculation of the modes of polymer solution injection into the boundary layer without any negative manifestations of the effects of the elastic deformations. The results of the numerical simulation confirmed the conception on the deformation-stress state of macromolecules (fluid elements) in polymer solution converging flow, based on the data previously obtained from experimental decisions concerning the hydrodynamic field structure in the input area of a slot and other openings.

Keywords: *polymer solution, Maxwell fluid, effect of elastic deformation, hydrodynamic field, velocity gradient, slot, Toms effect.*

2010 MSC: 76A10, 76M25　　　　　　　　　**DOI:** 10.23939/mmc2021.01.058

1. Introduction

Among the accepted methods of artificial impact on the boundary layer, aimed at reducing hydrodynamic resistance of friction the objects moving in the water, it is the method of supplying a water-soluble polymer where scientists have achieved the best practical advances [1–3]. Positive results obtained from experiments with objects moving in the water create the basis for research developments aimed at improving and upgrading systems supplying a polymer solution into the boundary layer; which, in particular, involves designing highly efficient compact plants for mixing a polymer solution directly at underwater crafts or floating facilities and supplying it into their boundary layer, without any noticeable deterioration in their overall design characteristics [2, 4–6].

However, after supplying the boundary layer of the streamlined objects with water-soluble polymers, the actual reduction of the friction resistance level is far from the results that were either theoretically predicted or obtained in the experiments with the same objects moving in a pre-prepared solution in a polymer pool [2, 5]. That restricts applying polymer additives on the moving in the water objects in order to reduce their friction resistance. Therefore, it is essential to address the technical issues aimed at increasing the velocity of underwater crafts or floating facilities and their energy efficiency by supplying a polymer solution into the boundary layer. That is primarily relevant for upgrading systems supplying polymer solutions into the boundary layer of the objects moving in the water.

In all experiments to our knowledge, the researchers have not yet sufficiently considered the hydrodynamics of polymer solutions that takes place in the constitutive elements of systems supplying the boundary layer of streamlined objects with polymer solutions. They believed that it was impossible to observe any significant 'anomalies' while the polymer solutions flow through slots or other openings; i.e. polymer solutions flowing into the boundary layer of the streamlined object, the hydrodynamic impact on the polymer system cannot have a noticeable influence on the Toms effect. Their conclusions based on the analysis of the data obtained during the study of shear laminar flows for which the elastic deformation effects are negligible [6].

In a typical hydraulic supplying system, as shown in [2,7], the flow is complex and combines a superposition of shear flow and predominantly longitudinal (stretching) flow. With such flows, the effects of the elastic deformation become so essential, that neglecting them results in polymer additives not being fully utilized, especially with objects moving in the water at high velocities [4]. Ultimately, that increase the polymer overrun costs and reduce its efficiency, therefore reducing the time the object moving in the water is in afterburning [2,5].

Hence, significant resources for increasing the efficiency of polymer systems are not limited only to developing and enhancing polymers [1,4,7] but should also concern improving supplying systems and optimizing hydrodynamic modes of polymer solution flow into the boundary layer of objects moving in the water [2,5,6]. It is proven in [2,5] that the correct choice of the supplying system design and hydrodynamic modes for polymer solution flow into the boundary layer of streamlined objects can increase the efficiency of the reducing turbulent friction by more than 25%, compared to previously obtained data.

Determining the optimal flow mode of the polymer solution in the supply systems is one of the most comprehensive challenges that must be dealt with when designing systems for supplying polymer to the boundary layer of streamlined objects with regards to the negative manifestation of the effects of elastic deformations. Hydrodynamic flow modes through the constitutive elements of the supplying system are calculated, based on the condition satisfying the inequality:

$$\dot{\varepsilon}\theta_c \leqslant \mathrm{De_{cr}}, \tag{1}$$

where θ_c is relaxation time of the polymer solution; $\dot{\varepsilon}$ is longitudinal velocity gradient [8–10].
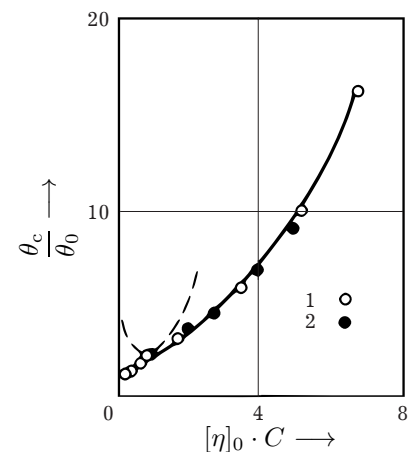
Expression (1) should be interpreted as the Deborah number because the inverse value of the longitudinal gradient of velocity is nothing but the time scale of the stream [8]. Thus, the calculation covers calculating the relaxation time (characteristic time) of the polymer solution and the longitudinal velocity gradient taking place in the outlet slot of the system supplying polymer to the boundary layer of the streamlined object. According to the experimentally obtained data, the critical Deborah number for water solutions of polyethylene oxide (PEO) is 2.5 [5].

We obtained the following equation to define the characteristic relaxation time of the polymer solution (viscoelastic fluid) (2) [10]:

$$\theta_c = \begin{cases} \theta_0 e^k & \text{at} \quad k < 1, \\ \theta_0 \dfrac{e^{k^{2/3}}}{k^{1/3}} & \text{at} \quad k > 1, \end{cases} \tag{2}$$

where $[\eta]_0$ is characteristic viscosity, C is concentration of polymer in solution, and $[\eta]_0 \cdot C = k$. Dependence θ_c/θ_0 on $[\eta]_0 \cdot C$ for PEO of two different molecular masses in the water as shown in Fig. 1.

Fig. 1. Profiles of θ_c/θ_0 for varying $[\eta]_0 \cdot C$ for different PEO concentration in solution, M_{PEO}: 1) $4 \cdot 10^6$, 2) $2.5 \cdot 10^6$.

The solid line shows the course of the dependence obtained for equation (2). We can see that the points obtained during the experiments for the corresponding concentration regions lie satisfactorily

on the estimated curve. So, substituting the known molecular characteristics of the polymer into equation (2) we can calculate the relaxation time of polymer solutions. The effect of temperature in this equation is taken into account by the temperature dependence θ_0 and k.

At the same time, research literature to our knowledge doesn't highlight any analytical equations for calculating a longitudinal velocity gradient in the input area of the slot in the system supplying polymer to the boundary layer of a streamlined object. To calculate the longitudinal velocity gradient of the polymer solution flow in the sub-slot chamber of the supplying system, it is necessary, taking into account its viscoelastic properties, to analyze the flow of the hydrodynamically active polymer solution through the slot.

2. Problem statement

Hydrodynamically active polymer solutions possess viscoelastic properties [11–13]. Therefore, when polymer solution flows through the slot, to evaluate deformation characteristics of the flow (stream functions, distributions of the longitudinal velocity gradient and normal stress) resulting in manifestation of abnormal (compared with the behaviour of the ordinary fluid) effects, we can use a well-known Maxwell's fluid model [11–14] with the Jaumann derivative [15].

We chose this model because, according to Lodge [14], the study of non-linear, non-permanent, from the view of Lagrange, currents of viscoelastic fluids doesn't add any new information to the already obtained by studying homogeneous or quasi-homogeneous shear deformations. In his opinion, "...the only reason for detailed calculations of different types of non-linear currents is to make sure that they are practically implemented." This Lodge's statement can be interpreted in such a way, that there is no need for new rheological equations to describe convergent flows (in the input area of the slot); it's enough to use the equations of a steady Couette flow [11], or, at least, to determine whether they can explain the features of the convergent flow in the sub-slot chamber of the system supplying polymer into the boundary layer of the object moving in the water.

3. Solution

To describe steady streamflow in the incompressible environments, we use the following classical equations [8, 15]:
– the continuity equation

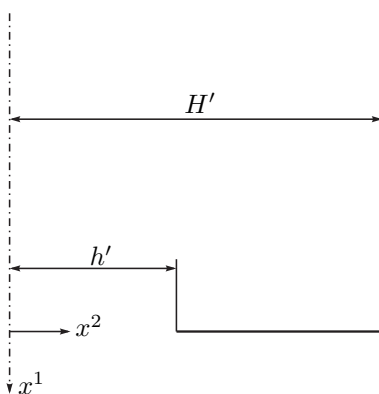$$\mathcal{V}^i_{,i} = 0, \tag{3}$$

– the Cauchy motion equation

$$\rho \mathcal{V}^k \mathcal{V}^i_{,k} = -g^{ik} P_{,k} + T^{ij}_{,k}, \tag{4}$$

where g^{ik} is metric tensor, and $T^{ij}_{,k}$ is determined by covariant differentiation T^{ij}:

$$T^{ij}_{,k} = \frac{\partial T^{ij}}{\partial x^k} + \left\{^i_{k\ m}\right\} T^{mj} + \left\{^i_{k\ m}\right\} T^{im},$$

where $\left\{^i_{k\ m}\right\}$ are the Christoffel symbols expressed by the dependence:

$$\left\{^i_{k\ m}\right\} = \frac{1}{2} g^{i\ell} \left(\frac{\partial g_{k\ell}}{\partial x^m} + \frac{\partial g_{m\ell}}{\partial x^k} - \frac{\partial g_{km}}{\partial x^\ell} \right).$$

Fig. 2. The shape of the slot and Cartesian coordinates.

Having designated θ_c to relaxation time and η_c — to viscosity, we can write the structural rheological equation of the Maxwell's fluid model [4, 11–13, 15, 16]:

$$T^{ij} + \theta_c \frac{D_j T^{ij}}{Dt} = 2\eta_c D^{ij},\tag{5}$$

where $\frac{D_j}{Dt}$ is the Jaumann derivative described by the equation

$$\frac{D_j T^{ij}}{Dt} = \frac{\partial T^{ij}}{\partial t} + \mathcal{V}^k T^{ij}_{,k} - W^i_k T^{kj} - T^{ik} W^j_k,$$

in which

$$D_{km} = \frac{1}{2}\left(\mathcal{V}_{k,m} + \mathcal{V}_{m,k}\right),$$

$$W_{km} = \frac{1}{2}\left(\mathcal{V}_{k,m} - \mathcal{V}_{m,k}\right).$$

Analyze the case, where the incompressible fluid moves between two parallel planes and flows through the slot which length is considerably longer than width. The flow is flat and stationary. Fig. 2 shows the shape of the slot of the sub-slot chamber of the system supplying polymer into the boundary layer of the streamlined object and Cartesian coordinates.

The components of the metric tensor in Cartesian coordinates are:

$$g_{11} = g_{22} = 1,$$
$$g_{12} = g_{21} = 0.$$

The Christoffel symbols $\left\{{}^i_{k\ m}\right\}$ equal zero since the components of the metric tensor g_{ik} are not coordinate-dependent. Let us express this in a dimensionless form, introducing the following quantities into equations (3), (4) and (5):

$$
\begin{aligned}
x_1^* &= \frac{x^1}{H'}, & x_2^* &= \frac{x^2}{H'},\\
V_1^* &= \frac{\mathcal{V}^1}{\bar{u}}, & V_2^* &= \frac{\mathcal{V}^2}{\bar{u}},\\
T_{11}^* &= \frac{H'}{\eta_c \bar{u}} T^{11}, & T_{22}^* &= \frac{H'}{\eta_c \bar{u}} T^{22},\\
T_{12}^* &= \frac{H'}{\eta_c \bar{u}} T^{12}, & T_{21}^* &= \frac{H'}{\eta_c \bar{u}} T^{21},\\
P^* &= \frac{H'}{\eta_c \bar{u}} P,
\end{aligned}
\tag{6}
$$

where $\bar{u}$ is average flow velocity; $2H'$ is slot width. Considering transformations (3), (4), (5), they are reduced to:

$$\frac{\partial \mathcal{V}_1^*}{\partial x_1^*} + \frac{\partial \mathcal{V}_2^*}{\partial x_2^*} = 0,\tag{7}$$

$$\mathrm{Re}\left(\mathcal{V}_1^* \frac{\partial \mathcal{V}_1^*}{\partial x_1^*} + \mathcal{V}_2^* \frac{\partial \mathcal{V}_1^*}{\partial x_2^*}\right) = -\frac{\partial P^*}{\partial x_1^*} + \frac{\partial T_{11}^*}{\partial x_1^*} + \frac{\partial T_{12}^*}{\partial x_2^*},\tag{8a}$$

$$\mathrm{Re}\left(\mathcal{V}_1^* \frac{\partial \mathcal{V}_2^*}{\partial x_1^*} + \mathcal{V}_2^* \frac{\partial \mathcal{V}_2^*}{\partial x_2^*}\right) = -\frac{\partial P^*}{\partial x_2^*} + \frac{\partial T_{21}^*}{\partial x_1^*} + \frac{\partial T_{22}^*}{\partial x_2^*},\tag{8b}$$

$$T_{11}^* + \text{We} \left\{ \mathcal{V}_1^* \frac{\partial T_{11}^*}{\partial x_1^*} + \mathcal{V}_2^* \frac{\partial T_{11}^*}{\partial x_2^*} - \frac{1}{2} \left(\frac{\partial \mathcal{V}_1^*}{\partial x_2^*} - \frac{\partial \mathcal{V}_2^*}{\partial x_1^*} \right) \left(T_{12}^* + T_{21}^* \right) \right\} = 2 \frac{\partial \mathcal{V}_1^*}{\partial x_1^*}, \tag{9a}$$

$$T_{22}^* + \text{We} \left\{ \mathcal{V}_1^* \frac{\partial T_{22}^*}{\partial x_1^*} + \mathcal{V}_2^* \frac{\partial T_{22}^*}{\partial x_2^*} + \frac{1}{2} \left(\frac{\partial \mathcal{V}_1^*}{\partial x_2^*} - \frac{\partial \mathcal{V}_2^*}{\partial x_1^*} \right) \left(T_{12}^* + T_{21}^* \right) \right\} = 2 \frac{\partial \mathcal{V}_2^*}{\partial x_2^*}, \tag{9b}$$

$$T_{12}^* + \text{We} \left\{ \mathcal{V}_1^* \frac{\partial T_{12}^*}{\partial x_1^*} + \mathcal{V}_2^* \frac{\partial T_{12}^*}{\partial x_2^*} + \frac{1}{2} \left(\frac{\partial \mathcal{V}_1^*}{\partial x_2^*} - \frac{\partial \mathcal{V}_2^*}{\partial x_1^*} \right) \left(T_{11}^* - T_{22}^* \right) \right\} = \frac{\partial \mathcal{V}_1^*}{\partial x_2^*} + \frac{\partial \mathcal{V}_2^*}{\partial x_1^*}, \tag{9c}$$

$$T_{21}^* + \text{We} \left\{ \mathcal{V}_1^* \frac{\partial T_{21}^*}{\partial x_1^*} + \mathcal{V}_2^* \frac{\partial T_{21}^*}{\partial x_2^*} + \frac{1}{2} \left(\frac{\partial \mathcal{V}_1^*}{\partial x_2^*} - \frac{\partial \mathcal{V}_2^*}{\partial x_1^*} \right) \left(T_{11}^* - T_{22}^* \right) \right\} = \frac{\partial \mathcal{V}_1^*}{\partial x_2^*} + \frac{\partial \mathcal{V}_2^*}{\partial x_1^*}, \tag{9d}$$

where $\text{Re} = \frac{\rho \bar{u} H'}{\eta_c}$ is the Reynolds number; $\text{We} = \frac{\theta_c \bar{u}}{H'}$ is the Weissenberg number.

If we restrict ourselves to a flow in which the inertial terms can be neglected, then the left side of equation (8) will equal zero. Applying the continuity equation (7), we introduce the stream function:

$$\mathcal{V}_1^* = \frac{\partial \psi}{\partial x_2^*}, \qquad \mathcal{V}_2^* = -\frac{\partial \psi}{\partial x_1^*}. \tag{10}$$

If we assume that the fluid flow at the supplying system input area has the Poiseuille velocity profile, the velocity on the surface of the solid wall (adhesion condition) equals zero, and the flow velocity is constant, the boundary conditions will take the following form:

$$x_1^* = -\infty, \quad \mathcal{V}_1^* = \frac{3}{2} \left(1 - x_2^{*2} \right), \quad \mathcal{V}_2^* = 0, \tag{11a}$$

$$x_1^* = 0, \quad 0 \leqslant x_2^* \leqslant h^*, \quad \mathcal{V}_1^* = \mathcal{V}_0^* \quad \mathcal{V}_2^* = 0, \tag{11b}$$

$$x_1^* = 0, \quad h^* \leqslant x_2^* \leqslant 1, \quad \mathcal{V}_1^* = \mathcal{V}_2^* = 0, \tag{11c}$$

$$x_2^* = 0, \quad \frac{\partial \mathcal{V}_1^*}{\partial x_2^*} = \mathcal{V}_2^* = 0, \tag{11d}$$

$$x_2^* = 1, \quad \mathcal{V}_1^* = \mathcal{V}_2^* = 0, \tag{11e}$$

where $\mathcal{V}_0^* = \text{const}$, determined by the expendable velocity; h^* is dimensionless value, equals $\frac{h'}{H'}$; $2h'$ is slot width.

It is necessary to solve equations (7), (8), and (9), according to the boundary conditions (11), to determine the flow and stress fields, according to the boundary conditions (11). It is not possible to solve these equations in a general form; therefore, we restrict ourselves to slow flows. In this case, we can not only neglect the inertial terms but also assume that the Weisenberg number is less than one.

Let us recall that the Weissenberg number characterizes the rate of the viscoelastic properties of the fluid in a shear flow. In the case under consideration, we have a complex flow with both shear and longitudinal velocity gradients. As the velocity of the outflow through the supply system slot increases, as proven in [7], the proportion of the longitudinal (stretching) flow increases, and the shear decreases. Therefore, it is more appropriate, instead of the Weissenberg number, to use a Deborah number, which characterizes the rate of viscoelastic properties in a stretching flow [8]. Nevertheless, for stationary flows, the ratio is $\frac{\text{De}}{\text{We}} = \text{Re}^{0.75}$ [8,17], which means that both criteria, We and De, are interconnected within geometrically similar flows.

Therefore, for restrictions, imposed on this flow, in the same way as in [15], we can write the velocities, stress, and stream functions as the decomposition by number We:

$$\begin{aligned}
\mathcal{V}_i^* &= \mathcal{V}_i^{(0)} + \text{We}\,\mathcal{V}_i^{(1)} + \text{We}^2 \mathcal{V}_i^{(2)} + \ldots, \\
P^* &= P^{(0)} + \text{We}\,P^{(1)} + \text{We}^2 P^{(2)} + \ldots, \\
T_{ij}^* &= T_{ij}^{(0)} + \text{We}\,T_{ij}^{(1)} + \text{We}^2 T_{ij}^{(2)} + \ldots, \\
\psi* &= \psi^{(0)} + \text{We}\,\psi^{(1)} + \text{We}^2 \psi^{(2)} + \ldots.
\end{aligned} \tag{12}$$

Substituting (12) into equations (7), (8), (9), and the boundary conditions (11), we will put the equation in order with respect to the Weissenberg number. Now we can write down the terms of equations that do not include the Weissenberg number:

$$\frac{\partial \mathcal{V}_1^{(0)}}{\partial x_1^*} + \frac{\partial \mathcal{V}_2^{(0)}}{\partial x_2^*} = 0, \tag{13a}$$

$$\frac{\partial T_{11}^{(0)}}{\partial x_1^*} + \frac{\partial T_{12}^{(0)}}{\partial x_2^*} = \frac{\partial P^{(0)}}{\partial x_1^*}, \tag{13b}$$

$$\frac{\partial T_{21}^{(0)}}{\partial x_1^*} + \frac{\partial T_{22}^{(0)}}{\partial x_2^*} = \frac{\partial P^{(0)}}{\partial x_2^*}, \tag{13c}$$

$$T_{11}^{(0)} = 2\frac{\partial \mathcal{V}_1^{(0)}}{\partial x_1^*}, \qquad T_{22}^{(0)} = 2\frac{\partial \mathcal{V}_2^{(0)}}{\partial x_2^*}, \tag{13d}$$

$$T_{12}^{(0)} = \frac{\partial \mathcal{V}_1^{(0)}}{\partial x_1^*} + \frac{\partial \mathcal{V}_2^{(0)}}{\partial x_1^*}, \tag{13e}$$

$$T_{21}^{(0)} = \frac{\partial \mathcal{V}_1^{(0)}}{\partial x_1^*} + \frac{\partial \mathcal{V}_2^{(0)}}{\partial x_1^*}, \tag{13f}$$

$$\mathcal{V}_1^{(0)} = \frac{\partial \psi^{(0)}}{\partial x_2^*}, \qquad \mathcal{V}_2^{(0)} = -\frac{\partial \psi^{(0)}}{\partial x_1^*}. \tag{13g}$$

Boundary conditions:

$$\begin{array}{llll}
x_1^* = -\infty, & \mathcal{V}_1^{(0)} = \frac{3}{2}\left(1 - x_2^{*2}\right) & \mathcal{V}_2^{(0)} = 0, & x_2^* = 0, \quad \frac{\partial \mathcal{V}_1^{(0}}{\partial x_2^*} = \mathcal{V}_2^{(0)} = 0, \\
x_1^* = 0, \quad 0 \leqslant x_2^* \leqslant h^*, & \mathcal{V}_1^{(0)} = \mathcal{V}_0^*, & \mathcal{V}_2^{(0)} = 0, & \\
x_1^* = 0, \quad h^* \leqslant x_2^* \leqslant 1, & \mathcal{V}_1^{(0)} = \mathcal{V}_2^{(0)} = 0, & & x_2^* = 1, \quad \mathcal{V}_1^{(0)} = \mathcal{V}_2^{(0)} = 0.
\end{array} \tag{14}$$

Considering equation (13), by expressing $\frac{\partial P^{(0)}}{\partial x_1^*}$, $\frac{\partial P^{(0)}}{\partial x_2^*}$ through $\psi^{(0)}$ and its derivatives and excluding $P^{(0)}$, we obtain:

$$\left(\frac{\partial^2}{\partial x_1^{*2}} + \frac{\partial^2}{\partial x_2^{*2}}\right)\psi^{(0)} = 0. \tag{15}$$

For boundary conditions (14) the solution of the equation (15) describes the flow of the ordinary fluid.

$$\psi^{(0)} = \psi^{(0)}\left(x_1^*, x_2^*\right).$$

By substituting equation (12) into equation (9) and grouping the terms with the Weissenberg number in the first power, we obtain:

$$T_{11}^{(1)} = \frac{1}{2}\left(\frac{\partial \mathcal{V}_1^{(0)}}{\partial x_2^*} - \frac{\partial \mathcal{V}_2^{(0)}}{\partial x_1^*}\right)\left(T_{12}^{(0)} + T_{21}^{(0)}\right) + 2\frac{\partial \mathcal{V}_1^{(1)}}{\partial x_1^*} - \mathcal{V}_1^{(0)}\frac{\partial T_{11}^{(0)}}{\partial x_1^*} - \mathcal{V}_2^{(0)}\frac{\partial T_{11}^{(0)}}{\partial x_2^*}, \tag{16a}$$

$$T_{22}^{(1)} = 2\frac{\partial \mathcal{V}_2^{(1)}}{\partial x_2^*} - \frac{1}{2}\left(\frac{\partial \mathcal{V}_1^{(0)}}{\partial x_2^*} - \frac{\partial \mathcal{V}_2^{(0)}}{\partial x_1^*}\right)\left(T_{12}^{(0)} + T_{21}^{(0)}\right) - \mathcal{V}_1^{(0)}\frac{\partial T_{22}^{(0)}}{\partial x_1^*} - \mathcal{V}_2^{(0)}\frac{\partial T_{22}^{(0)}}{\partial x_2^*}, \tag{16b}$$

$$T_{12}^{(1)} = \frac{\partial \mathcal{V}_1^{(1)}}{\partial x_2^*} + \frac{\partial \mathcal{V}_2^{(1)}}{\partial x_1^*} - \frac{1}{2}\left(\frac{\partial \mathcal{V}_1^{(0)}}{\partial x_2^*} - \frac{\partial \mathcal{V}_2^{(0)}}{\partial x_1^*}\right)\left(T_{11}^{(0)} - T_{22}^{(0)}\right) - \mathcal{V}_1^{(0)}\frac{\partial T_{12}^{(0)}}{\partial x_1^*} - \mathcal{V}_2^{(0)}\frac{\partial T_{12}^{(0)}}{\partial x_2^*}, \tag{16c}$$

$$T_{21}^{(1)} = \frac{\partial \mathcal{V}_1^{(1)}}{\partial x_2^*} + \frac{\partial \mathcal{V}_2^{(1)}}{\partial x_1^*} - \frac{1}{2}\left(\frac{\partial \mathcal{V}_1^{(0)}}{\partial x_2^*} - \frac{\partial \mathcal{V}_2^{(0)}}{\partial x_1^*}\right)\left(T_{11}^{(0)} - T_{22}^{(0)}\right) - \mathcal{V}_1^{(0)}\frac{\partial T_{21}^{(0)}}{\partial x_1^*} - \mathcal{V}_2^{(0)}\frac{\partial T_{21}^{(0)}}{\partial x_2^*}, \tag{16d}$$

where $\mathcal{V}_i^{(0)}$, $T_{ij}^{(0)}$ are the velocity and stress components of the terms of equations having the Weissenberg number in a zero power, respectively; they are known.

In the similar way, converting the continuity equation, the equation of motion and the boundary conditions, we obtain:

$$\frac{\partial \mathcal{V}_1^{(1)}}{\partial x_1^*} + \frac{\partial \mathcal{V}_2^{(1)}}{\partial x_2^*} = 0, \tag{17a}$$

$$\frac{\partial T_{11}^{(1)}}{\partial x_1^*} + \frac{\partial T_{12}^{(1)}}{\partial x_2^*} = \frac{\partial P^{(1)}}{\partial x_1^*}, \tag{17b}$$

$$\frac{\partial T_{21}^{(1)}}{\partial x_1^*} + \frac{\partial T_{22}^{(1)}}{\partial x_2^*} = \frac{\partial P^{(1)}}{\partial x_2^*}. \tag{17c}$$

Boundary conditions:

$$\begin{aligned}
x_1^* = -\infty, &\quad \mathcal{V}_1^{(1)} = \mathcal{V}_2^{(1)} = 0, \\
x_1^* = 0, &\quad \mathcal{V}_1^{(1)} = \mathcal{V}_2^{(1)} = 0, \\
x_2^* = 1, &\quad \mathcal{V}_1^{(1)} = \mathcal{V}_2^{(1} = 0, \\
x_2^* = 0, &\quad \mathcal{V}_1^{(1)} = \mathcal{V}_2^{(1)} = 0.
\end{aligned} \tag{18}$$

The stream function (10) takes the following form:

$$\mathcal{V}_1^{(1)} = \frac{\partial \psi^{(1)}}{\partial x_2^*}, \qquad \mathcal{V}_2^{(1)} = -\frac{\partial \psi^{(1)}}{\partial x_1^*}. \tag{19}$$

Considering (19) and excluding equation (17), we obtain this equation:

$$\left(\frac{\partial^2}{\partial x_1^{*2}} + \frac{\partial^2}{\partial x_2^{*2}} \right)^2 \psi^{(1)} = 0. \tag{20}$$

The solution of equation (20) with boundary conditions (18) has the form $\psi^{(1)} = 0$, consequently, the terms of the equation with the Weissenberg number in the first power do not affect the velocity distribution. However, as we can see from equation (16), stress $T_{11}^{(1)}$, $T_{22}^{(1)}$, $T_{12}^{(1)}$, $T_{21}^{(1)}$ prove the influence of the elasticity of the terms of the equation with the Weissenberg number in the first power. By substituting equation (12) into equation (19), taking into account that $\mathcal{V}_1^{(1)} = \mathcal{V}_2^{(1)} = 0$, and grouping the terms containing the Weissenberg number in the second power, we obtain:

$$T_{11}^{(2)} = 2\frac{\partial \mathcal{V}_1^{(2)}}{\partial x_1^*} + \frac{1}{2}\left(\frac{\partial \mathcal{V}_1^{(0)}}{\partial x_2^*} - \frac{\partial \mathcal{V}_2^{(0)}}{\partial x_1^*} \right)\left(T_{12}^{(1)} + T_{21}^{(1)} \right) - \mathcal{V}_1^{(0)}\frac{\partial T_{11}^{(1)}}{\partial x_1^*} - \mathcal{V}_2^{(0)}\frac{\partial T_{11}^{(1)}}{\partial x_2^*}, \tag{21a}$$

$$T_{22}^{(2)} = 2\frac{\partial \mathcal{V}_2^{(2)}}{\partial x_2^*} - \frac{1}{2}\left(\frac{\partial \mathcal{V}_1^{(0)}}{\partial x_2^*} - \frac{\partial \mathcal{V}_2^{(0)}}{\partial x_1^*} \right)\left(T_{12}^{(1)} + T_{21}^{(1)} \right) - \mathcal{V}_1^{(0)}\frac{\partial T_{22}^{(1)}}{\partial x_1^*} - \mathcal{V}_2^{(0)}\frac{\partial T_{22}^{(1)}}{\partial x_2^*}, \tag{21b}$$

$$T_{12}^{(2)} = \frac{\partial \mathcal{V}_1^{(2)}}{\partial x_2^*} + \frac{\partial \mathcal{V}_2^{(2)}}{\partial x_1^*} - \frac{1}{2}\left(\frac{\partial \mathcal{V}_1^{(0)}}{\partial x_2^*} - \frac{\partial \mathcal{V}_2^{(0)}}{\partial x_1^*} \right)\left(T_{11}^{(1)} - T_{22}^{(1)} \right) - \mathcal{V}_1^{(0)}\frac{\partial T_{12}^{(1)}}{\partial x_1^*} - \mathcal{V}_2^{(0)}\frac{\partial T_{12}^{(1)}}{\partial x_2^*}, \tag{21c}$$

$$T_{21}^{(2)} = \frac{\partial \mathcal{V}_1^{(2)}}{\partial x_2^*} + \frac{\partial \mathcal{V}_2^{(2)}}{\partial x_1^*} - \frac{1}{2}\left(\frac{\partial \mathcal{V}_1^{(0)}}{\partial x_2^*} - \frac{\partial \mathcal{V}_2^{(0)}}{\partial x_1^*} \right)\left(T_{11}^{(1)} - T_{22}^{(1)} \right) - \mathcal{V}_1^{(0)}\frac{\partial T_{21}^{(1)}}{\partial x_1^*} - \mathcal{V}_2^{(0)}\frac{\partial T_{21}^{(1)}}{\partial x_2^*}. \tag{21d}$$

Once in equations (17), (18) and (19) index (1) was substituted by (2), the continuity equations, the equations of motion, the boundary conditions and the stream function took the same form.

Therefore, excluding $P^{(2)}$, we obtain:

$$
\left(\frac{\partial^2}{\partial x_1^{*2}} + \frac{\partial^2}{\partial x_2^{*2}}\right)^2 \psi^{(2)} = \frac{\partial^2 \mathcal{V}_1^{(0)}}{\partial x_2^* \partial x_1^*}\left(\frac{\partial A}{\partial x_1^*} + \frac{\partial A}{\partial x_2^*}\right)
$$

$$
+ \frac{\partial \mathcal{V}_1^{(0)}}{\partial x_2^*}\left(\frac{\partial^2 A}{\partial x_1^{*2}} + 2\frac{\partial^2 T_{12}^{(1)}}{\partial x_2^* \partial x_1^*}\right) + \frac{\partial \mathcal{V}_2^{(0)}}{\partial x_1^*}\left(\frac{\partial^2 A}{\partial x_2^{*2}} - 2\frac{\partial^2 T_{12}^{(1)}}{\partial x_1^* \partial x_2^*}\right)
$$

$$
- C\frac{\partial^2 B}{\partial x_1^* \partial x_2^*} - \frac{B}{2}\left(2\frac{\partial^2 C}{\partial x_1^* \partial x_2^*} - \frac{\partial^2 A}{\partial x_2^{*2}} + \frac{\partial^2 A}{\partial x_1^{*2}}\right)
$$

$$
- \frac{\partial B}{\partial x_1^*}\left(\frac{\partial C}{\partial x_2^*} + \frac{\partial}{\partial x_1^*}\right) + \frac{\partial B}{\partial x_2^*}\left(\frac{\partial A}{\partial x_2^*} - \frac{\partial C}{\partial x_1^*}\right) + \frac{\partial^2 \mathcal{V}_1^{(0)}}{\partial x_2^{*2}}\cdot\frac{\partial T_{12}^{(1)}}{\partial x_1^*}
$$

$$
+ \frac{\partial^2 \mathcal{V}_2^{(0)}}{\partial x_2^{*2}}\cdot\frac{\partial T_{12}^{(1)}}{\partial x_2^*} - \frac{\partial^2 \mathcal{V}_1^{(0)}}{\partial x_1^{*2}}\cdot\frac{\partial T_{12}^{(1)}}{\partial x_1^*} - \frac{\partial^2 \mathcal{V}_2^{(0)}}{\partial x_1^{*2}}\cdot\frac{\partial T_{21}^{(1)}}{\partial x_2^*}
$$

$$
+ 2\frac{\partial \mathcal{V}_2^{(0)}}{\partial x_2^{*2}}\left(\frac{\partial^2 T_{12}^{(1)}}{\partial x_2^{*2}} + \frac{\partial^2 T_{12}^{(1)}}{\partial x_1^{*2}}\right) + \frac{A}{2}\left(\frac{\partial^2 B}{\partial x_2^{*2}} - \frac{\partial^2 B}{\partial x_1^{*2}}\right)
$$

$$
+ \mathcal{V}_1^{(0)}\left(\frac{\partial^3 T_{12}^{(1)}}{\partial x_2^{*2}\partial x_1^*} - \frac{\partial^3 T_{12}^{(1)}}{\partial x_1^{*3}} + \frac{\partial^3 A}{\partial x_1^{*2}\partial x_2^*}\right) + \mathcal{V}_2^{(0)}\left(\frac{\partial^3 T_{12}^{(1)}}{\partial x_2^{*3}} - \frac{\partial^3 T_{12}^{(1)}}{\partial x_2^{*2}\partial x_2^*} + \frac{\partial^3 A}{\partial x_2^{*2}\partial x_1^*}\right), \quad (22)
$$

where $A = T_{11}^{(1)} - T_{22}^{(1)}$; $B = \frac{\partial \mathcal{V}_1^{(0)}}{\partial x_2^*} - \frac{\partial \mathcal{V}_2^{(0)}}{\partial x_1^*}$; $C = T_{12}^{(1)} + T_{21}^{(1)}$.

Since the right-hand side of equation (22) is known, so by solving equation (22) that comprises the boundary conditions, we will obtain the terms of the equation with the Weissenberg number in the second power. These terms characterize the distribution of velocities and stresses. It should be noted that, in contrast to [15], the right-hand side of equation (22) contains derivatives of the order that is higher than in [15].

## 4. Results of the numerical simulation of the Maxwell fluid flow through the slot

Figures 3 and 4 visualise the stream function when ordinary (We = 0) and Maxwell (We = 0.1) fluids flow through the slot. Obviously, as the channel compression ratio decreases, the stream function experiences an increasing impact at the inlet slot.

When the Maxwell fluid flows through a simulated slotted chamber, there arises the circulation zone (Fig. 3b) which extends from the right corner of the channel to the slot and occupies a triangular area. The flow lines form the inlet flow. Consequently, a decrease in the channel compression ratio (as well as an increase in We) results in the input flooded jet.
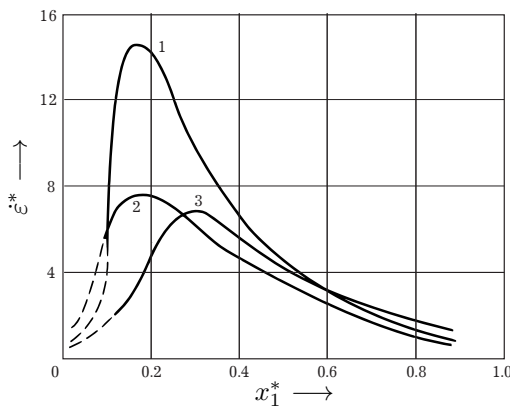

a ($h'/H' - 0.2$)   **b** ($h'/H' - 0.07$)
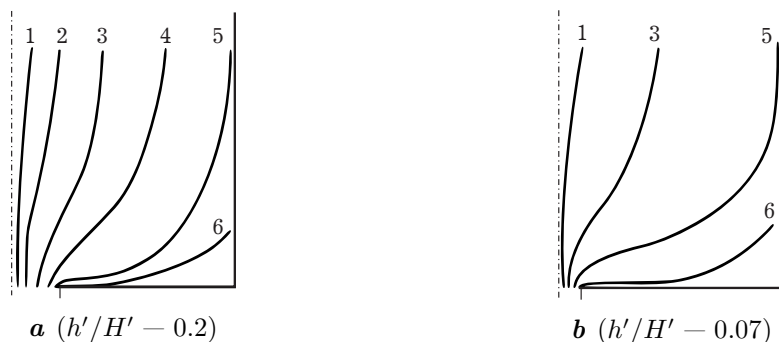
Fig. 3. The stream function, when flowing throughthe slot of the Newtonian fluid.
We = 0, Ψ: 1) 0.125, 2) 0.375, 3) 0.625, 4) 0.875, 5) 0.9715, 6) 1.0.
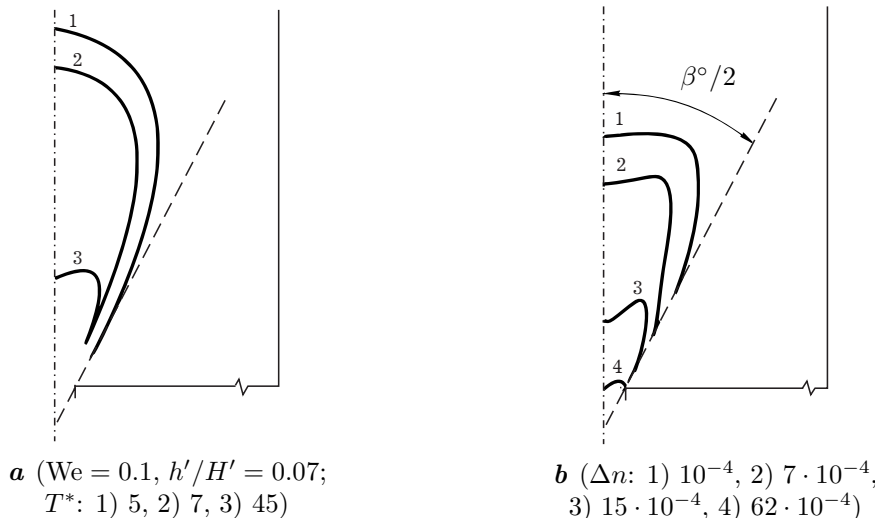
a $(h'/H' - 0.2)$ **b** $(h'/H' - 0.07)$
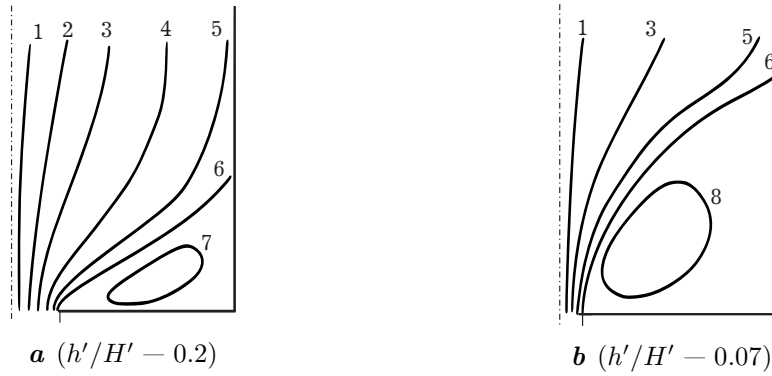
Fig. 4. The stream function, when flowing through the slot of the Newtonian fluid.
We = 0, Ψ: 1) 0.125, 2) 0.375, 3) 0.625, 4) 0.875, 5) 0.9715, 6) 1.0, 7) 1.01, 8) 1.1.

Fig. 5. The distribution of the dimensionless longitudinal velocity gradient along the axis of the fluid flowing into the slot. 1: $h'/H' = 0.07$, We = 0; 2: $h'/H' = 0.2$, We = 0; 3: $h'/H' = 0.2$, We = 0.1.

Fig. 5 shows the distribution of the dimensionless longitudinal velocity gradient along the flow axis when ordinary (curves 1 and 2) and Maxwell (curve 3) fluids flow into the slot. We can see that the maximum value of the velocity gradient in the flow of an ordinary fluid is reached at the distance $3h'$i $(x_1^* = 1.5)$ from the slot for the compression ratios of 0.2 and 0.07, respectively. The flowing fluid acquires the viscoelastic properties what shifts the maximum on the curve $\dot{\varepsilon}^* = f(x_1^*)$ to the region of large x^1 and decreases the value of $\dot{\varepsilon}_{\max}^*$.

A comparison of the experimental data obtained in [1, 7, 18, 19] with the results of the numerical simulations shows that the simulated flow lines and the distribution of the velocity gradient correspond to the experimentally obtained results for relatively low velocities.

a (We = 0.1, $h'/H' = 0.07$;   **b** (Δn: 1) 10^{-4}, 2) $7 \cdot 10^{-4}$,
T^*: 1) 5, 2) 7, 3) 45)   3) $15 \cdot 10^{-4}$, 4) $62 \cdot 10^{-4}$)

Fig. 6. The distribution of dimensionless normal stresses (a) and isochromes (b) in the input area of a slot. The angular half-width of the stream ($\beta^\circ/2$): 30°.

The distribution of dimensionless normal stress for the channel compression ratio of 0.07 and the Weissenberg number 0.1 is shown in Fig. 6.

The results properly visualise the experimental data on the distribution of isochromes in the input area of the slot (Fig. 6b and [20]). As in the polystyrene-bromoform system under consideration both the polymer and the solvent had the same refractive indices, the obtained lines of equal birefringence value (isochromes) inside the input flooded jet are proportional to the first difference of normal stresses.

Thus, the simulated flow lines, velocity fields and their gradients, as well as the distribution of stresses for ordinary and Maxwell fluids flowing through the slot, are at least qualitatively consistent with the available experimental data under the condition that we limit velocities to relatively low velocities. They are limited to the flow modes wherein elastic properties are just beginning to emerge.

In general, we should consider the entrance angle in the input area of the slot, by considering the problem in oblique or curved coordinate systems.

5. Conclusions

1. The obtained results prove that numerical simulation of the convergent Maxwell fluid flow can be used to calculate the longitudinal gradients in the input area of the slot of the system supplying polymer solution into the boundary layer of the object moving in the water.
2. The numerical analysis of the flow of the Maxwellian liquid through the slot is crucial for verifying and evaluating the experimental data characterizing the features of the converging flow of polymer solutions in the input area of a slot or other opening, as proposed in [6, 19].

[1] Pogrebnyak V. G., Pisarenko A. A. Solutions of Polymers under the Conditions of Wall Turbulence. Mechanism of Drag Reduction. International Journal of Fluid Mechanics Research. **29** (6), 779–797 (2002).

[2] Ivanyuta Yu. F. Experimental research of the influence of conditions of polymer admission to the boundary layer on reduction of turbulence friction. Inter. symposium on Seawater Drag Reduction, Newport, Rhode Island, 295–297 (1998).

[3] Povkh I. L., Toryanik A. I. Relation between molecular structure of polyethylene oxide solutions and drag reduction. Journal of Engineering Physics. **37** (4), 1131–1136 (1979).

[4] Pogrebnyak V. G., Naumchik N. V. On the hydrodynamic activity of polymers in high-velocity flows. Inzhenerno-Fizicheskii Zhurnal. **68** (1), 146–148 (1995), (in Russian).

[5] Povkh I. L., Ivanyuta Yu. F. Effekty uprugih deformatsiy pri podvode rastvora polimera na poverhnost obtekaemogo tela i snizhenie gidrodinamicheskogo soprotivleniya. Trudy po sudostroeniyu. Sektsiya V. Gidrodinamika sudov. TsNII im. akad. A. N. Krylova, Sankt-Peterburg, 299–306 (1994), (in Russian).

[6] Pisarenko A. A. Deformation effects in case of a flow with stretching of polymer solutions. Turbulence and Shear Flow Phenomena, in: S. Banerjee and J. K. Eaton (Eds.), Santa Barbara, California; New York, 1345–1350 (1999).

[7] Pogrebnyak A. V., Perkun I. V. Pogrebnyak V. G. Degradation of Polymer Solutions in a Hydrodynamic Field with a Longitudinal Velocity Gradient. Journal of Engineering Physics and Thermophysics. **90** (5), 1219–1224 (2017).

[8] Astarita J., Marucci J. Osnovyi gidromehaniki nenyutonovskih zhidkostey. Mir, Moscow (1978), (in Russian).

[9] De Gennes P. G. Coil-stretch thransition of dilute flexible polymers under ultrahigh velocity gradients. J. Chem. Phys. **60** (12), 5030–5042 (1974).

[10] Pogrebnyak A. V. Rozrahunok parametriv strumeneformuyuchoyi golivky dlya vodopolimernoyi obrobky materialiv rizannyam. Nauk. visnik Natsion. Lisotehnich. Univer: Uraine. Lviv. **27** (3), 187–190 (2017), (in Ukrainian).

[11] Vinogradov G. V., Malkin A. Ya. Reologiya polimerov. Khimiya, Moscow (1977).

[12] Ferri J. Vyazkouprugie svoystva polimerov. Inostr. lit., Moscow (1993), (in Russian).

[13] Kristensen R. Vvedenie v teoriyu vyazkouprugosti. Mir, Moscow (1994), (in Russian).

[14] Lodge A. S. Elastichnyie zhidkosti. Vvedenie v reologiyu konechnodeformiruemyih polimerov. Nauka, Moscow (1999), (in Russian).

[15] Nakamura K. Medlennoe istechenie vyazkouprugoy zhidkosti po konicheskomu kanalu. Senk'i kikay gakkay si. **31** (8), 49–55 (1978), (in Japanese).

[16] Voytkunskiy Ya. I., Amfilohiev V. V., Pavlovskiy V. A. Sb. nauch. tr. Leningr. korablestr. ins-t. **69**, 19–25 (1970), (in Russian).

[17] Hintse I. O. Turbulentnost. Mehanizm i teoriya. Phiz.-mat. Izdat., Moscow (1963), (in Russian).

[18] Pogrebnyak V. G., Ivanyuta Yu. F., Frenkel S. Ya. Structure of the hydrodynamic field and strain behavior of flexible makromolecules in convergent flow. Vysokomolekulyarnye Soedineniya. Seriya A. **34** (3), 133–138 (1992), (in Russian).

[19] Pogrebnyak A., Chudyk I., Pogrebnyak V., Perkun I. Coil-uncoiled chain Transition of Polyethylene Oxide Solutions. Chem. Chem. Technol. **13** (4), 465–470 (2019).

[20] Brestkin Yu. V., Amribakhshov A. A., Kholmuminov A. A., Frenkel S. Y. Razvorachivanie makromolekul pri shodyaschemsya techenii. Izv. AN UzSSR. Seriya phiz.-mat. nauk. **6**, 80–84 (1988), (in Russian).

Течія рідини Максвелла в системі підведення гідродинамічно-активного полімеру до приграничного шару обтічного об'єкта

Погребняк В. Г.[1], Погребняк А. В.[2], Перкун І. В.[1]

[1] *Івано-Франківський національний технічний університет нафти і газу,*
вул. Карпатська, 15, 76019, Івано-Франківськ, Україна
[2] *Університет митної справи та фінансів,*
вул. Володимира Вернадського, 2/4, 49000, Дніпро, Україна

Наведено результати чисельного моделювання течії максвеллівської рідини в системі підведення гідродинамічно-активного полімеру до приграничного шару обтічного об'єкта. Розглянуто випадок повільної течії, коли інерційними членами можна нехтувати, а швидкості, напруження і функції течії можна записати у вигляді розкладання за числом Вейсенберга та вважати, що число Вайсенберга менше одиниці. Встановлені особливості поведінки рідини Максвелла під час протікання з повздовжнім градієнтом швидкості та прояву при цьому ефектів пружних деформацій мають визначальне значення в розумінні процесів, які відбуваються в системі підведення полімерного розчину до приграничного шару обтічного об'єкта. Розуміння природи виникнення ефектів пружних деформацій в системі підведення дозволяє запропонувати гідродинамічний розрахунок режимів інжекції розчину полімеру на поверхню об'єкта без негативного прояву ефектів пружних деформацій. Результати чисельного моделювання підтвердили отримані з експериментальних рішень питань про структуру гідродинамічного поля у вхідній ділянці щілини і короткого капіляру уявлення про деформаційно-напружений стан макромолекул (елементів рідини) у збіжному потоці полімерного розчину.

Ключові слова: *розчин полімеру, максвеллівська рідина, ефекти пружних деформацій, гідродинамічне поле, градієнт швидкості, щілина, ефект Томса.*